ACS OMEGA

http://pubs.acs.org/journal/acsodf

Article

Study of the Pulse of Peristaltic Pumps for Use in 3D Extrusion Bioprinting

Sidney C. Gasoto,* Bertoldo Schneider, Jr., and João A. P. Setti

Cite This: *ACS Omega* 2022, 7, 24091−24101

Read Online

ACCESS | Metrics & More | Article Recommendations

ABSTRACT: Peristaltic pumps are used in healthcare for their ability to aseptically displace various fluids, including medium-density gels and suspended solids. However, they have the undesirable characteristic of pulsing at their output. Three-dimensional printing is becoming a reality in tissue engineering, and it generally uses syringes to extrude hydrogels. One of the problems to be solved is the microdosing of biomaterials or bioinks when it is necessary to print large volumes. The use of peristaltic pumps in bioprinting is desirable as it does not limit the volume to the contents of a syringe while achieving dosage control. A peristaltic pump was designed and implemented to avoid pulsation errors and microliter dosing while allowing a large amount of fluid displacement. Two pumps with equal displacement were built. The first uses the conventional profile and is the baseline for comparisons, while the second presents the profile studied and proposed. The concepts demonstrated by Bernoulli were used, fixing the height of a column of water, while the two pumps provide flow to the system asynchronously, allowing the reading of pressure as a function of the speed variation created by the pulsation of each pump. An approximately 100 times reduction in pulsation was observed during fluid displacement with the variance reduced from 2.64 to 0.025 s^2. The two pumps were also installed on a modified Ultimaker FDM 3D printer, and a standard for comparison was printed using a water-based hydrogel, corn starch, and corn-derived triglyceride, showing that the proposed pump improves the deposition quality of the material. Three-dimensional prints, tubes 20 mm in diameter by 8 mm in height and 0.7 mm in wall width, were also produced. Videos obtained show that the first pump was not able to print more than 4 mm in height, while the second prints the model with high quality and without deficiency. The results show that the new pump profile is able to provide a sufficiently constant volume for three-dimensional printing with excellent deposition control, building a simple object but difficult to obtain for a common peristaltic pump.

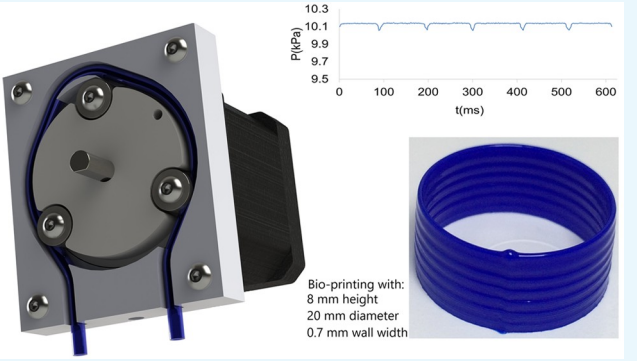

INTRODUCTION

Peristaltic pumps have excellent metering, sealing, asepsis, and easy maintenance characteristics. They do not require valves, and their mechanism has a long lifespan.[1] It can displace small suspended solids and low- and medium-density gels. They do not interact with mechanical parts and lubrication systems. These characteristics are beneficial for devices that promote the displacement of biomaterials for deposition in three dimensions, known as 3D bioprinters and other devices used in tissue engineering. In addition, the peristaltic pump has the potential to supply material derived from a reservoir, which can recharge during printing. The system allows printing large-volume objects;[2] it also can retract the product, which optimizes printing, removing excess and dripping during movements without biomaterial deposition. Bociaga et al.[2] showed that printers that use syringes for extrusion of biomaterials have reduced printing quality when the reservoir (syringe) assumes dimensions greater than 100 mL, which prevents the printing of whole organs, such as a liver, kidney, or heart. It also raises a crucial issue: the deposition of cells at the bottom of the reservoir by decantation. This problem can be solved with biomaterials agitation but is difficult to implement in syringe-type reservoirs. Bociaga et al.[2] presented the development of a 3D bioprinting system based on a peristaltic pump and tested two hydrogels with different compositions. This shows that the peristaltic pump has great importance in these devices, but it does not address the problem of pump pulsation.

Received: December 15, 2021
Accepted: May 30, 2022
Published: July 2, 2022

The term "peristaltic" refers to a tube's radial contraction and relaxation due to mechanical action or stimulus, moving along its length, forming a wave.[3,4]

This pump is suitable for low- and medium-viscosity biomaterials, such as air, liquids, gels, or suspensions, consisting of a liquid phase and a small dispersed solid phase. It is not indicated when the biomaterial consists of living cells if the occlusion is total. The tube suitable for a peristaltic pump applied in healthcare is silicone due to its asepsis characteristic.[1]

The housing is constructed so that the tube is inserted and withdrawn from the inner cylinder, forming an arc, and thus, the rollers restart the process. When a roller loses its action in the tube, it tends to expand, promoting the back-flow of the contained material, causing pulsation at the outlet.

The search for off-the-shelf peristaltic pumps provided many results, not shown here, with several manufacturers claiming that their pumps have low pulsation but without measuring this claim. In addition, they do not disclose their projects, making it impossible to evaluate and purchase a pump considered suitable for bioprinting.

Peristalsis is an effect found in most living things[5,6] and is widely used for pumping products. New publications show constant innovations in this type of pump. This work presents some of these publications. The objective is to evaluate the concepts and solutions of pulsation at the pump outlet, aiming at the extrusion of biomaterials in 3D printers. In some patents of peristaltic pumps found in this research, the authors claim to have low or no pulsation. This section will show these patents.

Lambert and Joergensen[1] showed a low-pulsation peristaltic pump system, Figure 1, with two lines of six rollers each offset by 30°, accommodating two interconnected tubes in the pump input and output by "Y" elements. Thus, the pulsation of one of the paths combines with the pulsation of the other, smoothing the pulses. However, it uses a lot of rollers and two tubes. This technique doubles the volume displaced per revolution and implies that the motor must work at a very low speed to displace low amounts of biomaterial, desirable in bioprinters, in addition to decreasing the resolution on the volume control, the same problem with having large syringes when using small exit holes, as discussed by Bociaga et al.[2]

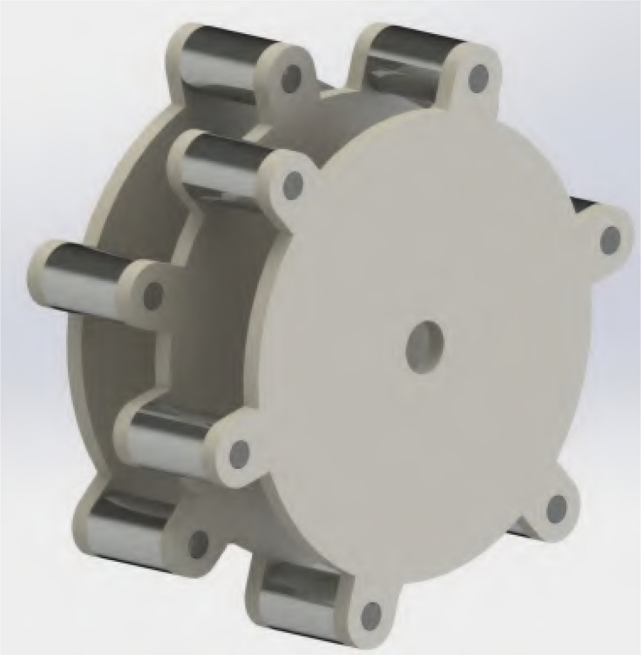

Figure 1. Lambert and Joergensen's pump. Two lines of six rollers each are shown offset by 30°.

Usually industries do not comment on their projects and do not disclose their secrets. However, Cole-Parmer (https://www.coleparmer.com/tech-article/reducing-pulsation-peristaltic-pumping) explained four methods to smooth pulsation at the output of their pumps. Almost all of these methods were studied in the patents presented, except the use of a pressure accumulator, called by them an air damper, as this method implies maintaining pressure in the output line through this accumulator, which makes it challenging to interrupt the flow in a controlled manner, which is unwanted in bioprinting.

In US patent 3,726,613,[7] the author uses a cam-controlled pusher synchronized with the drive, Figure 2. Rollers, or pistons, act on the wall of a flexible tube to compress at a location downstream of the elements, thus smoothing out pulsations in the flow of a fluid carried by the peristaltic pump. This element is gently removed during roller movement, reducing pulsation. It is a problematic construction device. It involves various moving components and exact sizing of the lever and cam. The fluid displacement caused by the pusher must be identical and synchronized with the displacement caused by the roller without obstructing the product outlet.

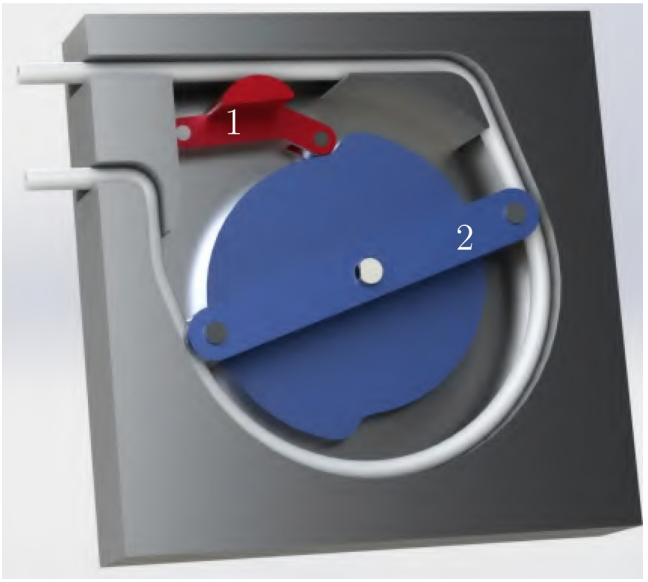

Figure 2. Casimir's pump. Pusher (1) displaces an equal volume as the roller (2).

It is possible to increase the flow accuracy of a peristaltic pump using multiple channels or tubes.[8] In his patent, US 4,673,344, the author described a pump with several spring cassettes split and pressed against a set of elongated rollers, Figure 3. These are mounted on a shaft, spaced evenly and circularly. Each cassette has a cam mounted on its side, which contacts the rollers and gradually relieves spring pressure on the installed tubes. The author states that these cams can be adjusted and replaced. This design makes it possible to adjust the flow rate and pulsation for different pipe diameters. The

https://doi.org/10.1021/acsomega.1c07093
ACS Omega 2022, 7, 24091−24101

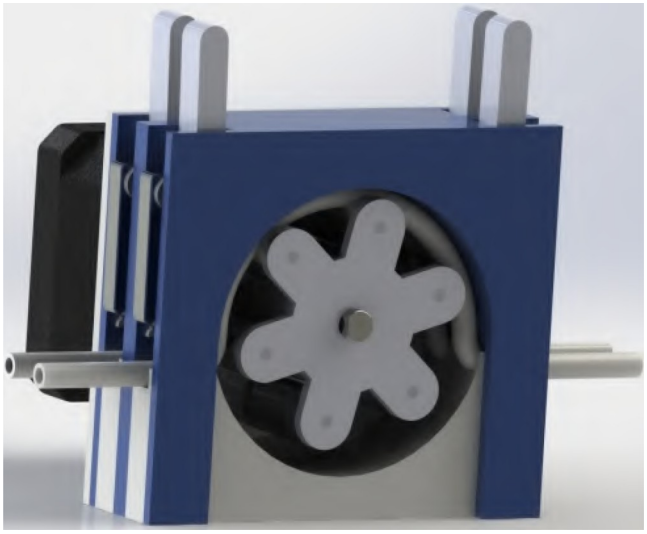

Figure 3. Allington's pump. Multiple channels with several spring cassettes.

author also claims that it is possible to replace cassettes and tubes while the pump is running.

In US patent 5,620,313,[9] the author described a peristaltic pump composed of 4 tubes arranged parallel to each other and between the rotor axis, Figure 4, in the form of an endless thread. The rotor compresses at least two distinct points, forming a volume inside the tube between each occlusion point that moves as a function of rotor rotation. The pump works with the effect of a linear peristaltic pump with the compression zone advancing along each tube from one end to the other, displacing the product along the tube. The author does not state how the contact between the rotor and the tubes occurs in the patent description. It is believed that there is friction between these elements, which would cause the tube to wear out rapidly. However, the displacement is continuous and sinusoidal, which minimizes pulsation if added to the output.

Another device[10] that eliminates the sudden entry and exit of rollers on the peristaltic pump tube, minimizing the volumetric pulse of its exit, has a rotor with three rollers and a spring system to push in the direction of occlusion of the tubes, Figure 5. However, a cam drives the rollers and moves them away from the tube continuously and gradually, providing a linear ramp. The system is divided into three sectors of 120°. Sectors S1 and S3 have a ramp that linearly presses the tubes, while in sector S2, the tube is pressed continuously, providing the occlusion and, therefore, the displacement of the fluid contained in the tube. This method does not eliminate the pulsation. It just distributes it, thus creating a nonlinear displacement of the fluid. Segment constriction causes nonlinearity in a pump cycle at the beginning of sector two and releases after the end of the same sector. This causes expansion of the tube and suction of the volume at the outlet.

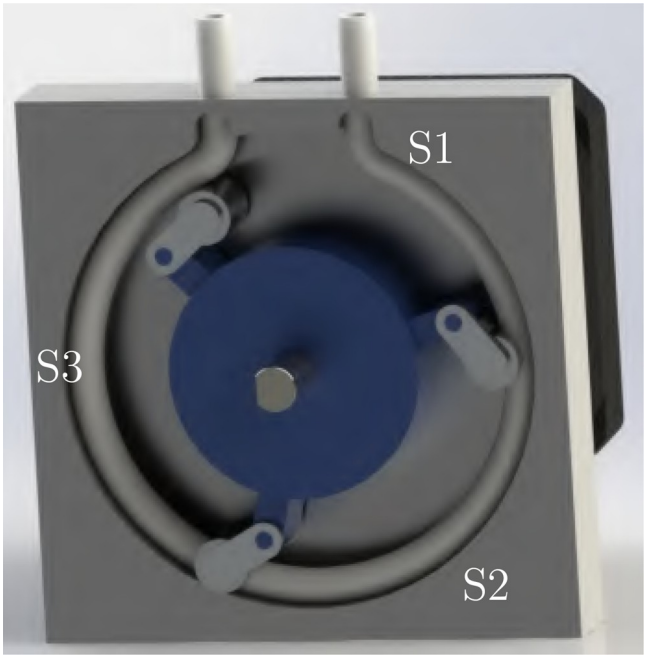

Figure 5. Pringle's pump. Cam drives the rollers and moves them away from the tube continuously and gradually, providing a linear ramp. System is divided into three sectors of 120°, S1, S2, and S3.

In US patent 2005/0084402 A1,[11] a device similar to that proposed by Pringle[10] was shown, Figure 6, basically differentiating the spring actuation system as it uses three rollers and a housing profile that resembles a cam divided into

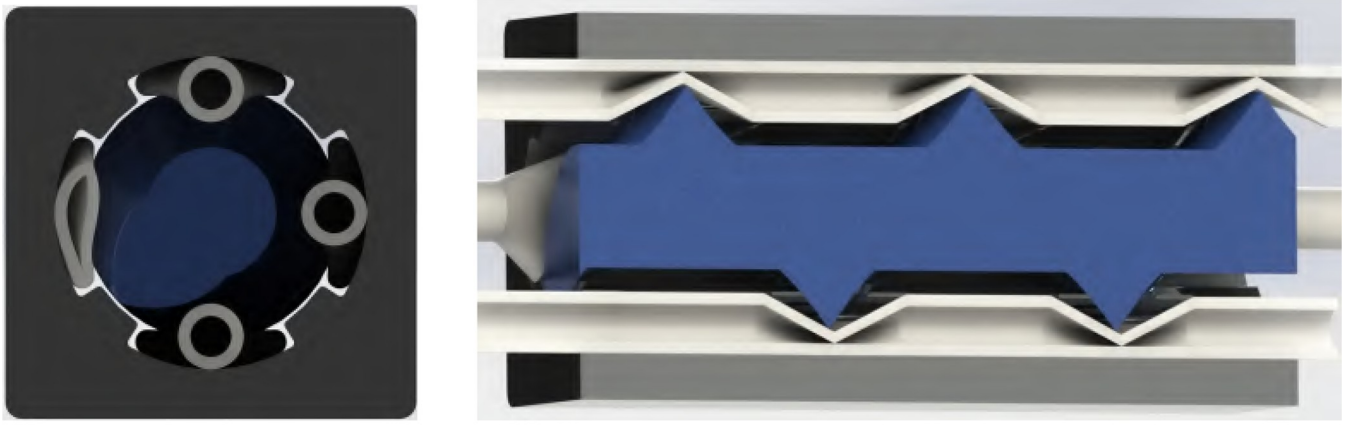

Figure 4. Fockenberg's pump. Four tubes are arranged parallel to each other and between the rotor axis. Radial (a) and axial (b) views.

https://doi.org/10.1021/acsomega.1c07093
ACS Omega 2022, 7, 24091−24101

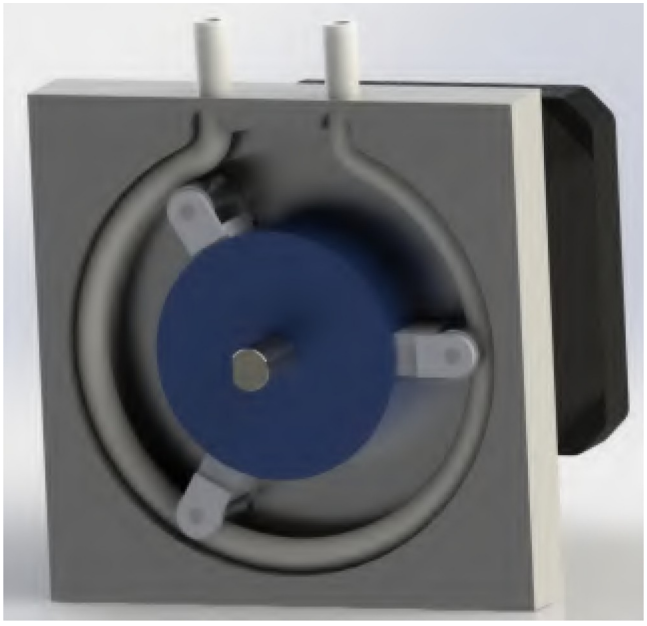

Figure 6. Vanek's pump uses three rollers and a housing profile that resembles a cam divided into sectors, which either presses or does not press the pump tube.

sectors, which either presses or does not press the pump tube. The authors argue that removing all of the pulsation from the pump is impossible. Even so, they guarantee that their design can linearize the dosage for one rotation of the rotor, making the occlusion area the same length as the release area of the tube, that is, 120°.

Two patents, US 8,079,836 B2 and JP 2007-298034 A,[12,13] presented a slight variation of the presented models with four rollers, Figure 7, and also defended the initial and final ramp in the occlusion region pulse smoothing.

Patent US 2006/0245964 A1[14] differs from the others. It includes a delayed occlusion relief of 120° from the pump outlet, Figure 8. When one roller relieves the tube, the other presses it, compensating for the effect of negative fluid displacement eliminating pulsation. The patent presents a variety of designs that try to cover as many pump models as possible, always with the same purpose of relieving occlusion lag at a certain distance depending on the number of rollers. It is the best solution found during the search. The patent remains valid, and reproduction for commercialization is not allowed.

The device is defended in EP 3 017 836 A1[15] in which the pipeline is placed in a cavity with four zones, Figure 9. The first zone is arranged so that a roller causes between 0 and 100% occlusion during movement. The second and third zones allow the roller to maintain total occlusion during travel. The fourth zone is constructed so that the roller gradually decreases occlusion during its movement. The length of each zone is less than the length of the arc between the two neighboring latching elements. The sum of the lengths of the second and third zones is equal to the distance of the bow between the two adjacent latching elements.

The cross-section of the tube is variable. In the second zone, the cross-section is larger than that in the third zone by an amount that leads to an increase in volume equal to that displaced in the fourth zone at the moment of disengagement from the pipe roll.[15] At first glance, the pump is the same as the others studied. However, the characteristic variation of the inner diameter of the tube sets it apart. It corrects the displaced volume, eliminates fluid back-flow, and ensures adequate dosage, but it is not easy to manufacture. The patent remains valid, and reproduction for commercialization is not allowed.

To facilitate understanding, Table 1 summarizes the patents and characteristics of interest to this research.

McIntyre et al.[16] evaluated the pulsation of a peristaltic pump through simulation and compared the results with a pump obtained by additive manufacturing. It applies pulsation measurement techniques with pressure sensors using standard valves for flow control to adjust the flow at the pump outlet. His work is rich in detail and demonstrates the simulated trials

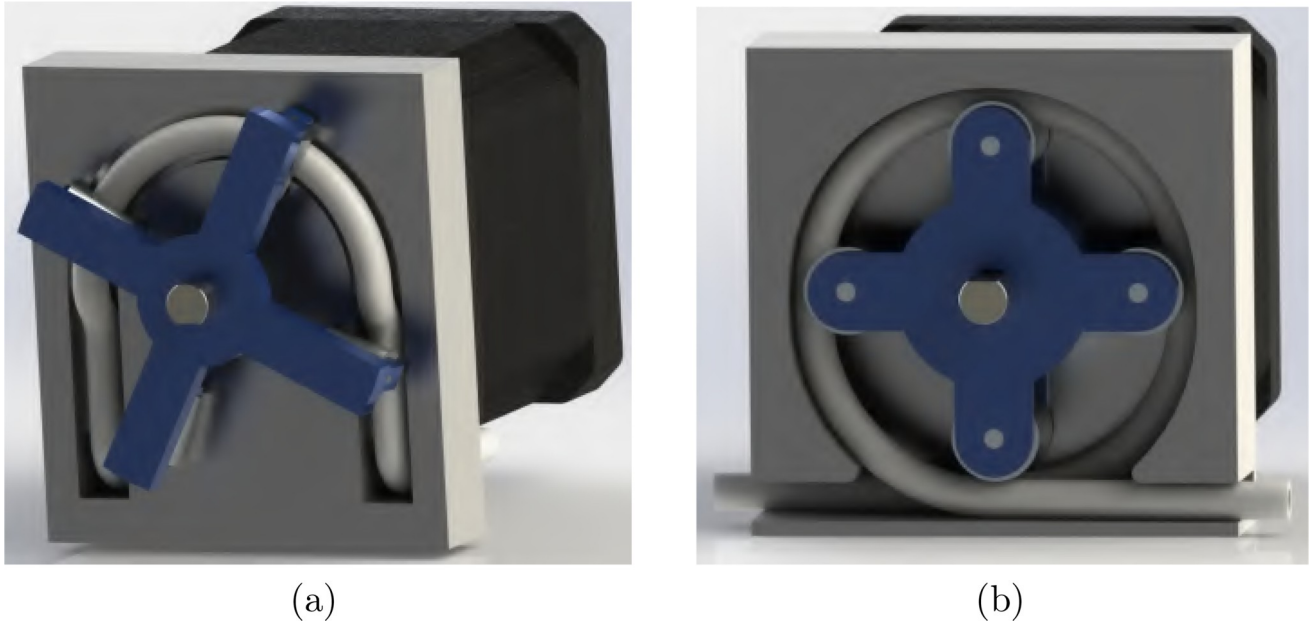

Figure 7. Gao and Oude's pump. Slight variation of the presented models with four rollers: (a) Gao's pump and (b) Oude's pump.

https://doi.org/10.1021/acsomega.1c07093
ACS Omega 2022, 7, 24091−24101

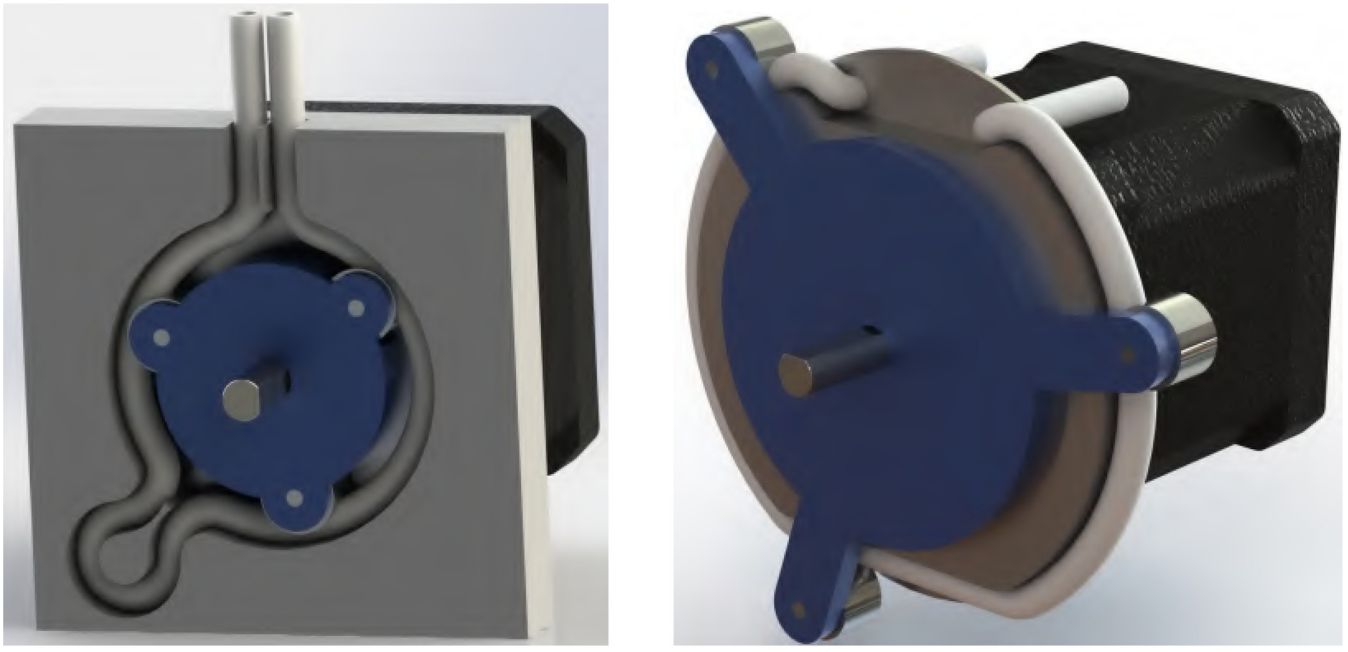

Figure 8. Koslov et al.'s pumps. Delayed occlusion relief of 120° from the pump outlet. Two designs (a and b) are shown.

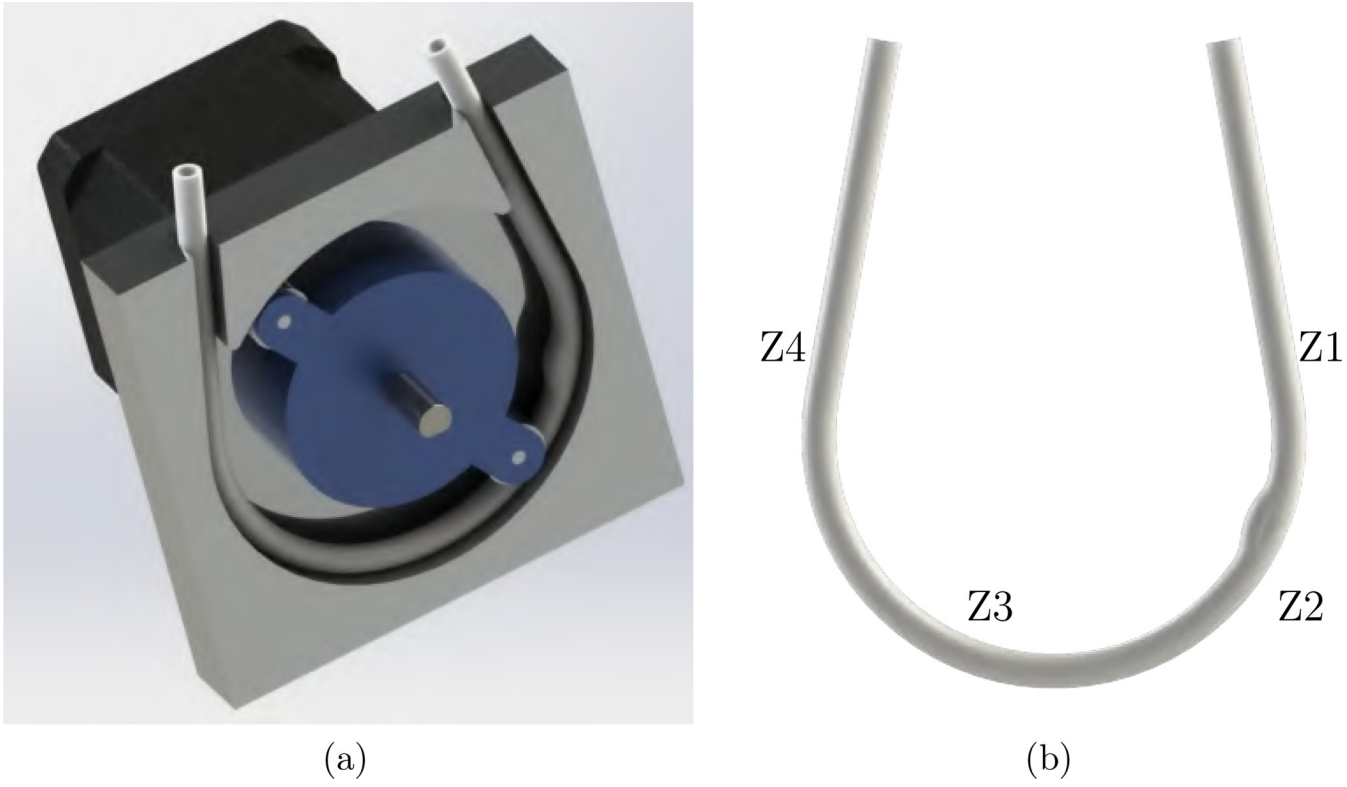

Figure 9. Tsoukalis's pump. Variation of the inner diameter of the tube: pump profile house (a) and tube profile(b).

of two- and three-roller pumps. The flow control valve used is simple and does not contain the necessary resources to keep the flow constant since, in this type of valve, when the pressure increases the flow also increases.

The elements used to dispense products on the printing base in bioprinters are like the needles used in healthcare but without the bevel, diagonal cut that provides better perforation capacity. They use the same Gauge (Ga) codes, color patterns, and beveled needle diameters (https://darwin-microfluidics.com/blogs/tools/syringe-needle-gauge-table). Each researcher must choose the appropriate model for their impression, hydrogel type, and viscosity.

For a satisfactory result, the ideal is that the outer diameter of the needle is equal to or greater than the width of the

https://doi.org/10.1021/acsomega.1c07093
ACS Omega 2022, 7, 24091−24101

Table 1. Summary of Patents

author	general characteristics
Lambert and Joergensen[1]	easy to build, pulses are minimized but not eliminated
von Casimir[7]	eliminates pulses but difficult to build
Allington and Hull[8]	minimizes pulses a lot but difficult to build, volume is multiplied by the number of tubes
Fockenberg[9]	minimizes pulses, difficult to build, volume is multiplied by the number of tubes, friction can shorten tube life
Pringle[10]	distributes pulses linearly but difficult to build, lots of moving elements, does not eliminate pulses
Vanek[11]	low pulse, easy build
Gao and Williams, Oude[12,13]	easy to build but does not eliminate pulses
Koslov et al.[14]	easy to build, eliminates pulses completely
Tsoukalis[15]	eliminates pulses completely

desired printed stroke, that is, a 0.4 mm needle will make a stroke up to 0.4 mm wide, while the height is defined by the distance from the needle tip to the previous layer. For the trace to have the desired height and width profile, a continuous material flow must be provided and defined by the printing speed and the displacement of the pump. A line 0.5 mm wide by 0.3 mm high and 1 mm long will have a volume of 0.15 mm^3 of material, or 0.15 μL. Therefore, for the print speed of 600 mm/min, the material flow should be 90 mm^3/min. The best print results were obtained when the maximum height was limited to 75% of the width. In this way, it is possible to calculate the flow required for each needle model and printing speed.

MATERIALS AND METHODS

When one wants to deposit small amounts of material, as is the case with 3D bioprinting, any difference in the dosed volume can represent an unwanted form of printing, causing a lack or excess of biomaterial. Bioprinters need the biomaterial deposited during printing to be supplied continuously in a uniform volume. Pulses cause media to supply failures that affect printing. The pulsation occurs due to the material reflux in the expansion region. When the roll is removed, the rolling volume is shifted back into the tube.[4] For each complete revolution of the rotor, there will be several back-flow pulses equal to the number of rollers, and the frequency (in Hertz) is given by the number of rollers multiplied by the rotor speed (in rpm), given by eq 1

$$\text{freq} = \frac{\text{no. of rollers} \times \text{rotor speed}}{60} \quad (1)$$

The volumetric flow, defined as the volume of a fluid that crosses a specific area per unit time for peristaltic pumps,[17] is given in cm^3/min by

$$Q = 0.5 \times \pi^2 \times d^2 \times N \times r \quad (2)$$

where d is the inner diameter (in cm) of the flexible tube, N is the rotational speed (in rpm), and r (in cm) is the radius of the chamber, measured from the center of the rotor shaft to the center of the roller that presses the tube.

The volumetric flow rate can be expressed in terms of the parametric factors of the peristaltic pump. From eq 2, it can be stated that for a given size of the flexible tube in the peristaltic pump, the flow depends not only on the speed of rotation but also on the radius of rotation.[17]

Determining the ideal flow for a peristaltic pump applied to a bioprinter depends on several factors, from the viscosity of the biomaterial, the desired wall width, and the speed at which you want to print, not being an easy task. The authors decided on a flow rate that they believe is sufficient for most low-viscosity fluids and gels and reasonable printing speed, ranging from 52.947 μL/min to 1,058.947 mL/min.

It has been proposed to manufacture two pumps containing characteristics of those studied, including overlapping some of them. The first pump (pump A) has the characteristics of the pump proposed by Oude.[13] However, it is intended to be the baseline with only three rolls. As seen in Figure 10, the cavity

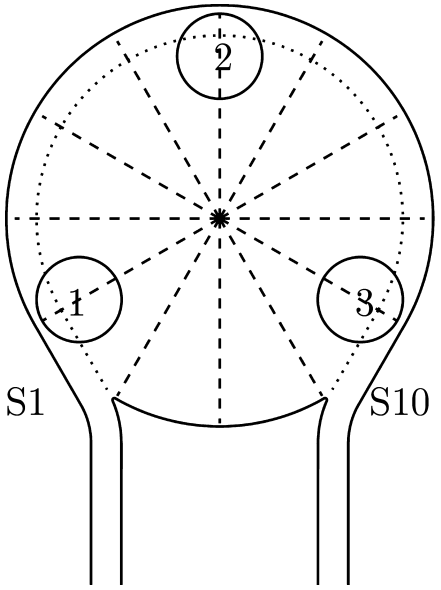

Figure 10. Profile of the first pump produced. When the rotation is clockwise, the 3rd roller moves over the 10th section (S10) and the pipe cleaning movement occurs in the form of a ramp created by the arc region in this section. On the other hand, the other rollers keep it pressed, moving the biomaterial toward the exit and continuing the movement. Third roller again presses the tube in the first section (S1), also in the form of a ramp created by the arc in this region, forming a volume between rollers 3 and 1, which is continuously displaced while the rotor turns.

circumference was divided into 12 sections of 30° each. During the rotating movement of the rotor, the rollers are moved simultaneously. When the rotation is clockwise, the 3rd roller moves over the 10th section (S10) and the tube clearing movement occurs in the form of a ramp created by the arc region in this section. On the other hand, the other rollers keep it pressed, moving the biomaterial toward the exit and continuing the movement. The third roll presses the tube again in the first section (S1), also in the form of a ramp created by the arc in this region, forming a volume between rolls 3 and 1, which is continuously displaced while the rotor rotates.

The second pump (pump B) was built using the concepts found in Koslov, Hagen, and Koslov.[14] However, ramps were made in sections S1, S4, S6, and S10 and the pipe deviation along section S5, Figure 11.

Removal of the roller from the S10 section causes an increase in the volume of the tube. However, as the volume of the material moved between two rollers is constant, this causes the material to retract, causing the pulsation to appear at the

https://doi.org/10.1021/acsomega.1c07093
ACS Omega 2022, 7, 24091−24101

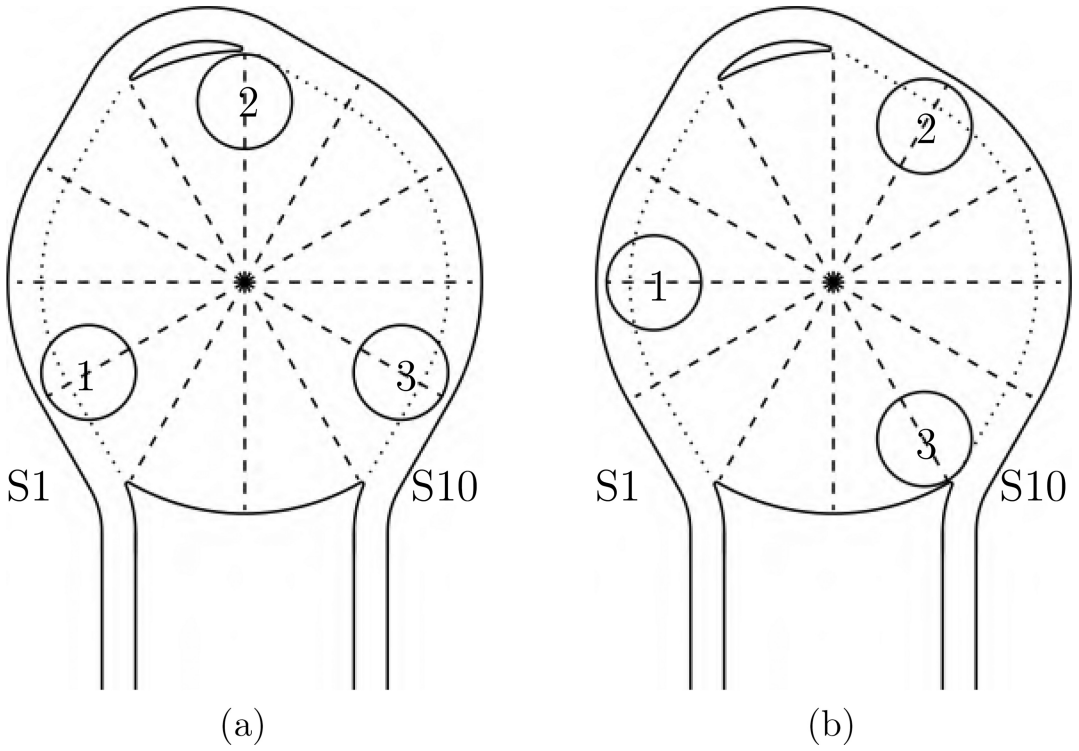

Figure 11. Profile of the second pump produced. Different pump times. (a) At T0, roll 1 is in total occlusion, roll 2 is at the beginning of occlusion, while roll 3 is at the beginning of release. (b) At T1, roll 1 is wholly occluded, roll 2 at the end of the ramp is already occluded, and roll 3 at the end of the ramp is entirely unobstructed.

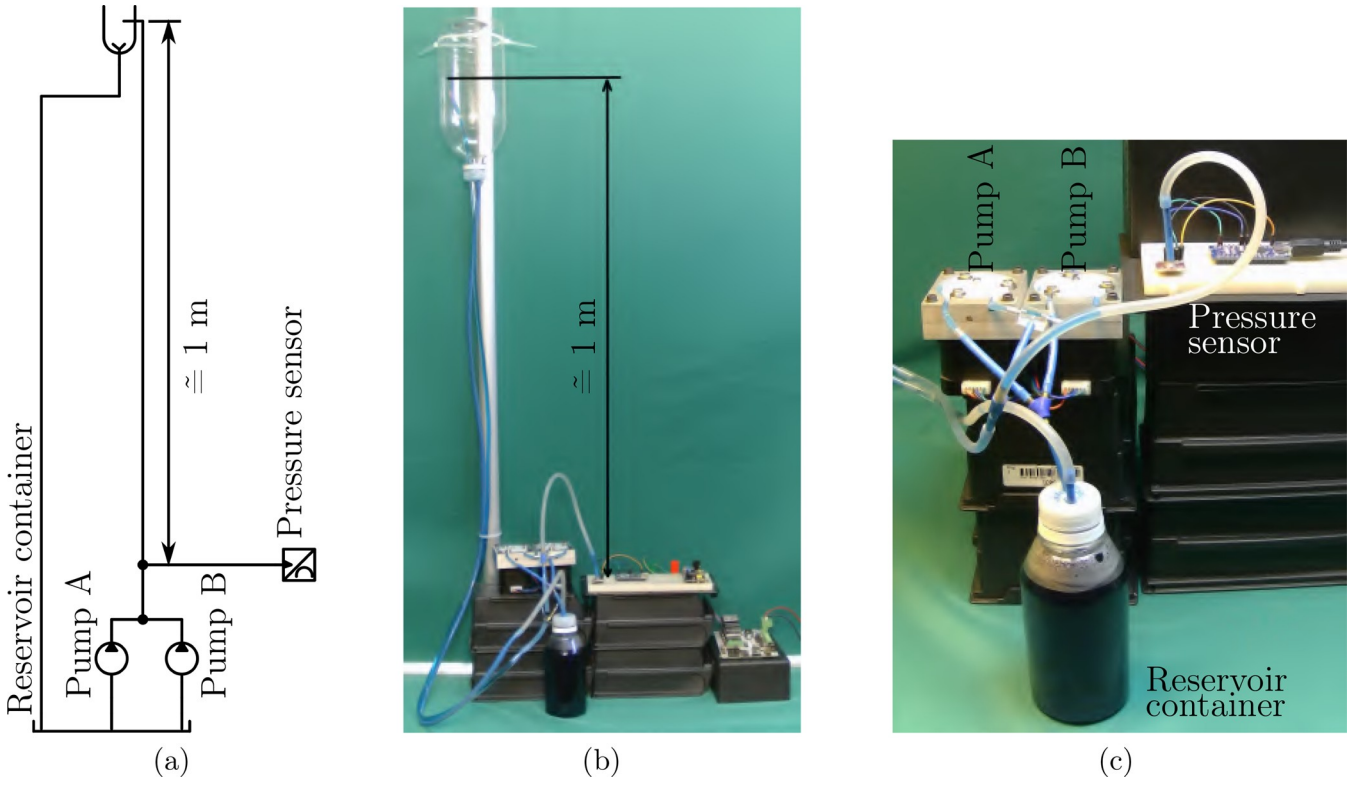

Figure 12. Assembly for pump pulsation tests. (a) Piping schematic. (b) Photo of the assembled system. (c) Detailed photo showing the pumps, sensor, and reservoir.

product outlet. Removing the previous roller, section 4, before closing the roller in section 1 causes more material to be introduced into the tube, creating a larger volume between the two rollers between sections 1 and 9. When clogging the tube in section 2, the release of the roller at S10 begins simultaneously with the reintroduction of the roller into

https://doi.org/10.1021/acsomega.1c07093
ACS Omega 2022, 7, 24091−24101

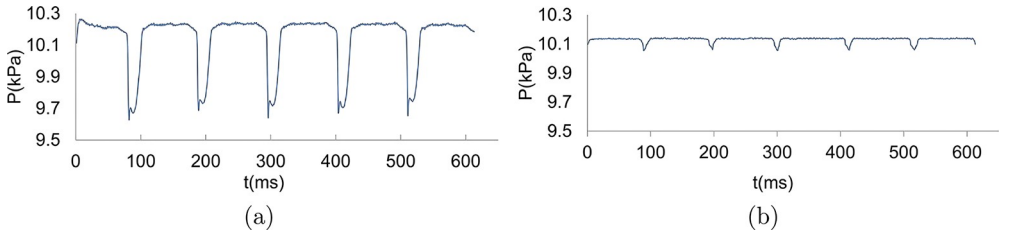

Figure 13. Graph obtained by reading the pressure sensor: (a) pump A and (b) pump B.

section S6 in a linear fashion, correcting the expansion movement of the tube on the roller at S10, since the roller at S6 presses the tube in the same proportion as it is withdrawn at S10.

For the pump displacement analysis, the following data are applied in eq 2

- inner diameter of the tube d = 1 mm = 0.1 cm
- number of rotor rotations N = 1
- roll center radius r = 1.7167 cm

$$Q(\mathrm{cm}^3) = 0.5 \times \pi^2 \times 0.1^2 \times 1.7167 = 0.08471(\mathrm{cm}^3) = 84.71\ (\mathrm{mm}^3) \quad (3)$$

The drive settings are set to

$$\mathrm{Var} = \mathrm{steps/mm}^3 = >3200/84.71 = 37.7759 \quad (4)$$

The 3D print configure file in the 3D printer extrusion adjustment variable is set to 37.3359.

The pumps were manufactured in a CNC with an aluminum body, the rotor in Poly-Oxy-Methylene (POM). The rollers are steel bearings with external and internal diameters of 9 mm and 5 mm, respectively. Each bearing has a width of 3 mm, and to allow compression of the tube, two bearings side by side were used. The pumps are driven by Nema 17, 4.5 kgf/cm stepper motors, controlled by the 3D printer board used for the experiment.

Pump Pulse Test. The two pumps were built and mounted side by side with the outputs connected in parallel and driven one at a time. The inlets were also joined in parallel and connected to a fluid reservoir. A dye was used to facilitate the observation of fluid displacement within the clear tube.

The displaced fluid was brought to a pressure sensor through a tube approximately 1.0 m above the pressure sensor, positioned vertically, opened, and installed inside a fluid collection system that takes it back to the reservoir. The height was adjusted to 10 kPa above the local atmospheric pressure, as indicated by the sensor when the pipe was filled with water at room temperature, and the pumps were turned off. According to the International System of Units (SI), 10 kPa is the pressure of 101.95 cm of the water column at 4 °C applied to a surface. This method guarantees a constant pressure in the system since when pumped the liquid exits through the upper end of the vertical tube, keeping the volume constant and, therefore, the pressure constant.

Figure 12 shows the circuit of the system.

The proposed test concept, which defines that the system pressure is constant if the flow is constant, can be expressed as

$$\frac{P}{\gamma} + \frac{v^2}{2} + gZ = \text{constant} \quad (5)$$

where P is the pressure, γ is the specific weight of the water contained in the vertical pipe, v is the velocity of the flow generated by the pump, g is the gravity acceleration, and Z is the height at which the water column is raised.

The flow is reversed when the roller unlocks the tube, and the velocity changes too, resulting in less pressure and allowing the pulsation to be observed with the sensor used. In Figure 12b and 12c the assembly details are shown. The proposed test allows the verification of small flow variations due to the sensor's sensitivity. The pressure sensor module for Arduino using BMP280 (https://www.bosch-sensortec.com/media/boschsensortec/downloads/datasheets/bst-bmp280-ds001.pdf) can measure pressures between 30 and 110 kPa with a 175 Hz sampling rate and 0.000 16 kPa resolution. This sensor is used to measure variations in atmospheric pressure and indicates the absolute atmospheric pressure at sea level. The experiment reads the local atmospheric pressure and subtracts this value from the measurements obtained, resulting in the relative value of the water column in the sensor.

The sensor module does not have a pipe connection. A metallic tube was installed over it with an adequate diameter for installing flexible tubes. A flexible membrane consisting of a PVC film was used over the sensor to prevent it from coming into contact with the liquids and provided a good seal.

An Arduino Nano module was programmed with the necessary routine to read the sensor and send the data to the PC via USB serial. A Python application was built on the PC to read the data and save it, from which the graphs in Figure 13 were extracted. The motors were driven by a module containing the necessary electronics for operation. Two complete turns were commanded for each motor. The reading corresponds to the signal generated by the sensor during motor revolutions. The initial pressure of 10 kPa is due to the tube being filled with water. Therefore, there is constant pressure before starting the motors.

Printing with Pumps. The use of peristaltic pumps in a 3D printing system for biomaterials requires regular dosing along the path of the rollers. Two pumps were installed to replace the extrusion head of an Ultimaker 3D printer built by the author. The body of a 5 mL syringe was used as a reservoir for the product to be deposited on the glass platform covered with a thin layer of white PVC self-adhesive film, allowing for contrast during filming and photos. The piping between the reservoir and the pump was a silicone tube with an external diameter of 4 mm and an internal diameter of 1 mm. The pump tube was silicone with outside and inside diameters of 4 and 1 mm, respectively. The rest of the tubing was rigid and transparent, ending in a Luer Lock fitting, ensuring better sealing and fixing, where a 22 Ga needle without bevel was placed. The material used for printing was a hydrogel composed of 200 mL of water, 10 g of corn starch, and 5 mL of triglyceride derived from corn. The mixture was heated to boiling. Blue food coloring was used to obtain better contrast in the photos and videos. The mixture was

https://doi.org/10.1021/acsomega.1c07093
ACS Omega 2022, 7, 24091−24101

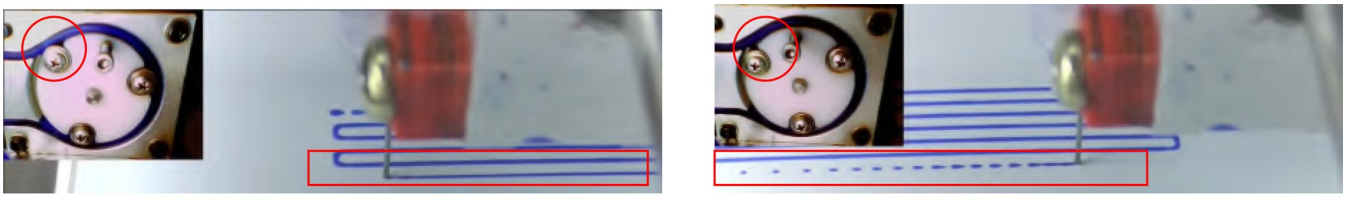

(a) (b)

Figure 14. Printing with pump A. Images were taken from the video of pump A at the moment when the roller starts releasing the tube due to the start of the ramp ((a) time 00:00:33:19) and at the end of the ramp ((b) time 00:00:38:27). It is possible to observe that until the beginning of the ramp the trace is consistent. Rectangle in a surrounds the region, and along the ramp, the stroke loses its width until complete absence, surrounded by the rectangle in b. Circles indicate the roll positions at the beginning and end of the print failure.

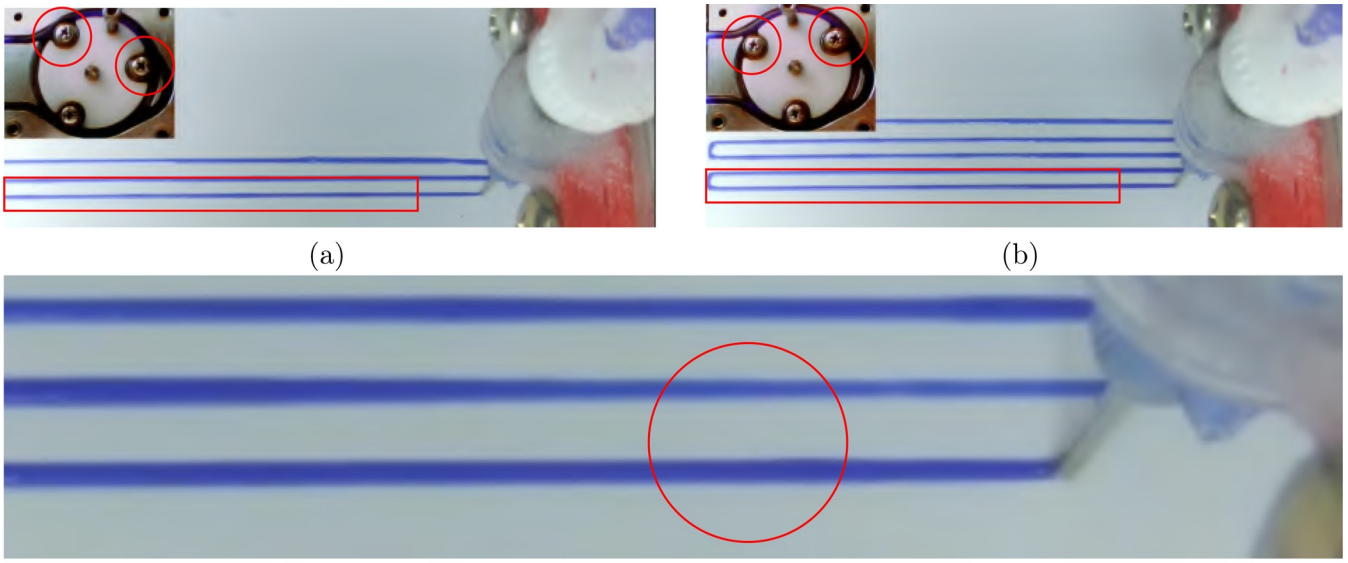

(a) (b) (c)

Figure 15. Printing with pump B. Images taken from the video of pump B at the moment when the ramp starts to release the tube (a) and at the end of the ramp (b). Rectangles that enclose the print regions in a and b show the regularity of the stroke width during the roll exit ramp over the tube. Circles in a and b indicate the timing between the last and the second to last rolls. (c) It is possible to see a slight decrease in the thickness of the line.

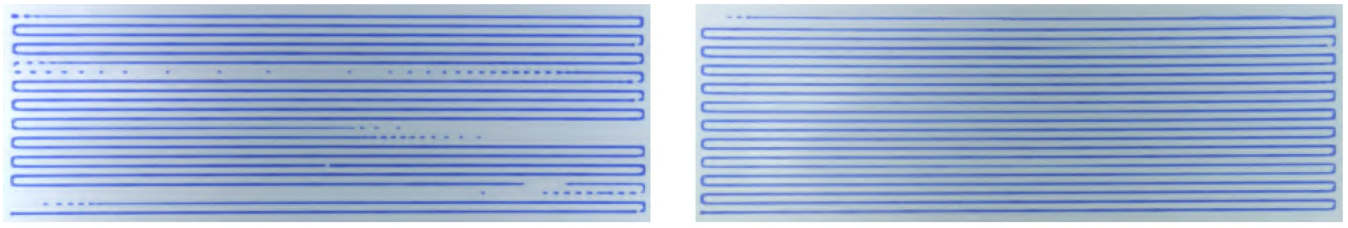

(a) (b)

Figure 16. Photo of prints; In (a) Pump A, there is a lack of material in some places; In (b) Pump B, it is possible to see a slight decrease in the line thickness.

homogenized and cooled to room temperature before use. Two cameras filmed the tests. One pointed at the printing base and the other at the pumps. All of the photos, video, gcode used for printing, and the data file obtained can be found on GitHub (https://github.com/sidneygasoto/Peristaltic-pump-3D-print/).

The videos were edited to reduce the time and file size and accelerated three times. The Repetier-Host (https://www.repetier.com/) app was used to control the 3D printer. Figures 14 and 15 show the results of material deposition with peristaltic pumps A and B, respectively.

It is possible to observe the printing faults and the variation of the stroke width for pump A, while in pump B, no faults are observed; only a slight decrease in the stroke width is observed, seen in more detail in Figure 16.

RESULTS AND DISCUSSION

In the graph of Figure 13 it is possible to see that the pressure peaks for each roller unclog the tube and return to occlusion. Table 2 shows the statistical calculations obtained from the sensor reading presented in the .xlsx file.

https://doi.org/10.1021/acsomega.1c07093
ACS Omega 2022, 7, 24091−24101

Table 2. Results of Statistical Calculations Obtained by Sampling

	pump A pressure (kPa)	pump B pressure (kPa)
maximum	10.264	10.144
minimum	9.629	10.056
medians	10.225	10.137
standard deviation	0.164	0.0159
variations (s^2)	2.68	0.025

A gcode has been edited to print a line whose length requires more than one turn of the pump impeller, allowing checking the rollers passing through the areas causing the failure.

Equation 5 was used to determine the pump's displacement to obtain the necessary volume of product to be deposited during the impressions. Pump displacement is a parameter used to configure the printer and defines the number of pulses in the stepper motor for each mm^3 of product.

The gcode (https://github.com/sidneygasoto/files/standardpattern.ngc) (line 12) defines that the printer should print from the current location (X = 65.00 and Y = 15.00, defined in the previous line) to X = 65.00 and Y = 150 0.00, that is, a straight line with a length of 135 mm in the Y direction, depositing 18.9 mm^3 of material during the path at a speed of 500 mm/s, 0.14 mm^3/min, which gives us an approximate height of 0.2 mm in the line when using the 22 Ga needle (~0.7 mm in diameter).

The same code was used to print on both pumps and can be seen in the Pump1-pattern.mp4 and Pump2-pattern.mp4 files found on GitHub (https://github.com/sidneygasoto/Peristaltic-pump-3D-printvideos). Figure 16 shows a photo of the prints obtained and the lack of material can be observed during the printing with Pump A, while with Pump B, no such failure is observed, only slight variations in the width of the trace.

A gcode (https://github.com/sidneygasoto/files/circle.ngc) was edited to print a 3D model; a tube of 20 mm in diameter and 8 mm in height, a single wall of approximately 0.7 mm in thickness, since a 22 Ga needle (~0.7 mm in diameter) was used. The same code was used to print using the two pumps, the exact product extrusion parameters, and the same hydrogel, and care was taken regarding the ambient temperature, printer leveling, and any other variables that could interfere with the experiment and can be seen in the videos Pump1-printing.mp4 and Pump2-printing.mp4 found on GitHub (https://github.com/sidneygasoto/Peristaltic-pump-3D-print), represented in Figure 17. From pump A, Figure 17a, one can observe the irregularity of the biomaterial deposition, creating a nonuniform face and collapsing after approximately 10−20 layers of 0.2 mm. Conversely, Figure 17b shows the print with pump B. It is observed that the variation in the width of the stroke, obtained in the experiment of printing the strokes, did not represent significant failures in the layered printing since there was no lack of sufficient material to interrupt the printing of the wall.

Notably, a literature search revealed only one method to investigate the pulsation of peristaltic pumps, which motivated the authors to apply the concepts found in Bernoulli's equation, eq 5, presented in this research, and to propose the method used for the use of both the sensor and the water column technique to maintain constant pressure during the experiment. The results obtained demonstrate consistency with those presented by the authors, showing the pulses at the time of removal of the rollers, proving the effect of flow reversal for pump A, while for pump B, a reduction in these pulses was attained, and the profile pump B allows the use of these for microdosing. During 3D printing with a higher viscosity biomaterial, pump B had displacement variation during the revolution. However, it still allowed an excellent result in the printed form, which suggests that it can be used for this purpose. The silicone tube was proposed because it is an inert material and consolidated use in the medical environment as a biocompatible product. However, it proved unsuitable for measuring high-viscosity materials as it expands when pressure is increased. To avoid this effect, further research with other materials for the tube is suggested, especially tubes with reinforced walls. Future work also suggests printing more complex 3D models, dimensional lifting of the printed models, and exhaustive tests with different biocompounds to obtain a

Figure 17. Photo of 3D prints: (a) 3D print 1 and (b) 3D print 2. Best results from five prints of each model. Irregularity of the deposition of the biomaterial can be observed (a), creating a face, not uniform. (b) Regular faces and near-perfect printing are obtained.

https://doi.org/10.1021/acsomega.1c07093
ACS Omega 2022, 7, 24091−24101

list of printable biomaterials using a peristaltic pump and needle system for controlled and precise control deposition.

CONCLUSION

Pulsation in peristaltic pumps can lead to wrong dosages due to the back-flow of product displaced from tube expansion when the element producing the occlusion is removed. The analysis of several pump models proposed in articles and patents showed that some models that can eliminate pulsation and therefore dosing errors. The work evaluated some models of pumps and submitted them to flow tests, obtaining the volume variation as a function of the pulsation. The use of a manometer and a set of vertical tubes was proposed to obtain constant pressure and compare two pumps built for this purpose. The first pump was built with ramps at the inlet and outlet of the rollers, which served as a benchmark, which resulted in a pressure variation of 2.68 s^2. On the other hand, the second pump, built with the concepts and optimizations of a studied model, produced a variance of 0.025 s^2. The pumps were installed on an Ultimaker 3D printer, and print images were obtained. It is possible to observe the absence of material caused by the removal of the roller over the tube in pump A, while in pump B, this phenomenon did not occur, showing that the pulsation was reduced. Thus, it is evident that it is possible to use peristaltic pumps to pump fluids in 3D bioprinters and other devices that require precise dosages. Pump B shows a reduction in the width of the trace, indicating that there was less deposition of the biomaterial. This effect was not relevant in the three-dimensional printing with the proposed biomaterial, maintaining the expected quality and uniformity. However, the author suggests the use of a silicone tube with thicker or reinforced walls, which prevents the tube from expanding at higher pressures, which occurs when the biomaterial has a higher density or the outlet diameter is small, the printing of more complex 3D models, dimensional lifting of the printed models, and exhaustive tests with different biomaterials.

AUTHOR INFORMATION

Corresponding Author

Sidney C. Gasoto − *Graduate Program in Electrical and Computer Engineering, Federal Technologic University of Paraná, Curitiba Paraná, Brazil;* orcid.org/0000-0003-2380-2981; Email: sidneygasoto@utfpr.edu.br

Authors

Bertoldo Schneider, Jr. − *Graduate Program in Electrical and Computer Engineering, Federal Technologic University of Paraná, Curitiba Paraná, Brazil*

João A. P. Setti − *Graduate Program in Biomedical Engineering, Federal Technologic University of Paraná, Curitiba Paraná, Brazil*

Complete contact information is available at: https://pubs.acs.org/10.1021/acsomega.1c07093

Author Contributions

The manuscript was written through contributions of all authors. All authors have given approval to the final version of the manuscript.

Funding

This research did not receive any specific grant from funding agencies in the public, commercial, or not-for-profit sectors.

Notes

The authors declare no competing financial interest.

REFERENCES

(1) Lambert, P.; Joergensen, F. Accurate dispensing of biopharmaceuticals. *World Pumps* **2008**, *2008*, 22−24.
(2) Bociaga, D.; Bartniak, M.; Sobczak, K.; Rosinska, K. An Integration of a Peristaltic Pump-Based Extruder into a 3D Bioprinter Dedicated to Hydrogels. *Materials* **2020**, *13*, 4237.
(3) Orchard, B. Laboratories and industry provide opportunities for peristaltic pumps. *World Pumps* **2004**, *2004*, 24−26.
(4) Hoffmeier, K. L.; Hoffmann, D.; Feller, K.-H. A first inherently pulsation free peristaltic pump. *Int. Wiss. Kolloq. - Technol. Univ. Ilmenau* **2014**, *58*, 11.
(5) Acharya, S.; Kou, W.; Halder, S.; Carlson, D. A.; Kahrilas, P. J.; Pandolfino, J. E.; Patankar, N. A. Pumping Patterns and Work Done During Peristalsis in Finite-Length Elastic Tubes. *J. Biomech. Eng.* **2021**, *143* (7), 071001.
(6) Khan, A. A.; Rafaqat, R. Effects of radiation and MHD on compressible Jeffrey fluid with peristalsis. *J. Therm. Anal. Calorim.* **2021**, *143*, 2775−2787.
(7) von Casimir, W. Pulsefree peristaltic pump. US Patent US 1973/3726613, 1973.
(8) Allington, R. W.; Hull, J. D. Peristaltic pump. US Patent US 1987/4673334, 1987.
(9) Fockenberg, K. Worm pump for flowable media. US Patent US 5,620,313, 1997.
(10) Pringle, J. T. Linearized peristaltic pump. US Patent US 2002/6413059 B1, 2002.
(11) Vanek, J. Peristaltic rotation pump with exact, especially mechanically linear dosage. US Patent US 2005/0084402 A1, 2005.
(12) Gao, S. X.; Williams, D. L. Method of operating a peristaltic pump. US Patent US 2011/08079836 B2, 2011.
(13) Oude, V. R. H. H. Peristaltic Pump. US Patent US 2007/0258829 A1, 2007.
(14) Koslov, A. P.; Hagen, L.; Koslov, A. P. Pulseless peristaltic pump. US Patent US 2010/7645127 B2, 2010.
(15) Tsoukalis, A. Pulseless rotary peristaltic pump. European Patent EP 3017836 A1, 2016.
(16) McIntyre, M. P.; van Schoor, G.; Uren, K. R.; Kloppers, C. P. Modelling the pulsatile flow rate and pressure response of a roller-type peristaltic pump. *Sens. Actuators, A* **2021**, *325*, 112708.
(17) Rao, P. S.; Reddy, G. B.; Reddy, V. D. Design and Development of Advanced Rotary Peristaltic Pump. *Int. J. Mater. Eng. Technol.* **2017**, *8*, 695−703.

https://doi.org/10.1021/acsomega.1c07093
ACS Omega 2022, 7, 24091−24101